Sensing and Bio-Sensing Research 3 (2015) 98–104

Contents lists available at ScienceDirect

Sensing and Bio-Sensing Research

journal homepage: www.elsevier.com/locate/sbsr

Amorphous silicon photosensors integrated in microfluidic structures as a technological demonstrator of a "true" Lab-on-Chip system

Domenico Caputo [a,*], Annalisa de Angelis [a], Nicola Lovecchio [a], Augusto Nascetti [b], Riccardo Scipinotti [a], Giampiero de Cesare [a]

[a] Department of Information Engineering, Electronics and Telecommunications, "Sapienza" University of Rome, via Eudossiana 18, Rome, Italy
[b] Department of Astronautics, Electrical and Energy Engineering, "Sapienza" University of Rome, via Salaria 851/881, 00138 Rome, Italy

ARTICLE INFO

Keywords:
Electrowetting
On-chip detection
Amorphous silicon photosensor
Microfluidics
Lab-on-Chip

ABSTRACT

In this paper we present a compact technological demonstrator including on the same glass substrate an electrowetting-on-dielectrics (EWOD) system, a linear array of amorphous silicon photosensor and a capillary-driven microfluidic channel. The proposed system comprises also a compact modular electronics controlling the digital microfluidics through the USB interface of a computer. The system provides therefore both on-chip detection and microfluidic handling needed for the realization of a 'true' Lab-on-Chip.

The geometry of the photosensors has been designed to maximize the radiation impinging on the photosensor and to minimize the inter-site crosstalk, while the fabrication process has been optimized taking into account the compatibility of all the technological steps for the fabrication of the EWOD system, the photosensor array and the microfluidics channels.

As a proof of the successful integration of the different technological steps we demonstrated the ability of the a-Si:H photosensors to detect the presence of a droplet over an EWOD electrode and the effective coupling between the digital and the continuous microfluidics, that can allow for functionalization, immobilization and recognition of biomolecules without external optical devices or microfluidic interconnections.

1. Introduction

In the early 1990's the introduction of the concept of the micro Total Analysis Systems (μTAS) and the development of micro-electro-mechanical technologies led to the development of Lab-on-Chip (LoC) systems as a powerful tool for complex chemical or bio-chemical analysis. A variety of recent technological breakthroughs in the fabrication of thin film physical and optical sensors have made possible the development of LoC systems where several functional modules are integrated onto a single substrate [1–3].

Each module has a specific function in the sample-treatment chain, such as: sample handling performed by a microfluidic system [4,5]; detection and quantification of biomolecules by using specific sensors [6].

Microfluidic devices are capable to handle fluid volume smaller than pico-liter scale through channels with dimensions of a few microns, but they often need macro-to-micro interconnections between micro-channels and external pumps. On the other hand, the electrowetting-on-dielectric (EWOD) technique leads to fluidic operations varying the shape of an electrically conductive liquid droplet by means on an external electric field [7–9], and may be an effective alternative to microchannels.

Detection modules rely often on thin film devices [10–13]. In particular hydrogenated amorphous silicon (a-Si:H) based devices, which can be utilized as physical [14], electronic [15] and optical devices [16], have received a lot of attention by different research groups, for optical biomolecule detection, both in labeled [17–19] and label-free [20]; [21] techniques, such as stimulated fluorescence detection [22,23], optical absorption measurements [24] and chemiluminescence detection [25–27].

The combination of microfluidics with analytic systems and detection is still the main bottleneck for a high miniaturization of the final device, and requires a fabrication process, which takes into account the compatibility between different materials and different technologies.

In this paper we present a solution for this drawback integrating, on a single glass substrate, amorphous silicon photodiodes with a fluid handling system performed by an electrowetting-on-

* Corresponding author.
E-mail address: caputo@die.uniroma1.it (D. Caputo).

http://dx.doi.org/10.1016/j.sbsr.2014.10.010
2214-1804/

dielectric (EWOD) module and a capillary-driven microfluidic channel, for achieving a technological demonstrator of a compact, stand-alone LoC system. In this way we avoid the use external pumps and/or syringes for movement as well as the use of external detectors and external optics to focus the emitted light, achieving a 'true' Lab-on-Chip system [28], where the only external component in our system is the front-end electronics that provides signal readout, driving voltages as well as power supply using a single USB connection of a laptop or PDA. In particular, Section 2 reports the description and the operation of the integrated system; Section 3 presents the design of the microfluidic system and of the a-Si:H photosensors; Section 4 reports the structure of the electronic board that controls and interfaces the microfluidic system with a computer in order to achieve the droplet movement in the EWOD system; Section 5 describes the steps sequence of the fabrication process of the LoC on a glass substrate, taking into account the compatibility of all the techniques used to fabricate the EWOD electrodes, the a:Si:H photosensors and the capillary-driven microchannels; Section 6 demonstrates the functionality and successful integration of the different fabrication processes. Finally, conclusions are drawn.

2. Description and operation of the system

Fig. 1 reports a cross section of the technological part of the proposed system. It includes:

- A linear array of transparent thin film electrodes (made in Indium Tin Oxide, ITO), fabricated on one side of a glass substrate and covered by an insulating and hydrophobic layer (polydimethylsiloxane, PDMS).
- A linear array of amorphous silicon (a-Si:H) photosensors, aligned with the transparent electrodes and fabricated on the other side of the same glass substrate.
- A capillary-driven microchannel placed at the end of the EWOD device and fabricated in PDMS by soft lithography process.

The amorphous silicon (a-Si:H) photosensors are aligned with both the EWOD device and the microchannel.

The photosensors aligned with the EWOD device monitor the presence of the droplet at the inlet of the microchannel and/or monitor, in specific sites of the EWOD device, the bio-chemical reactions that can be performed as sample pre-treatment before the liquid droplet is injected in the microchannel for the complete analysis. Indeed, the presence of the liquid droplet over the electrode can cause a variation of the light impinging on the photosensors that induces a variation of the photocurrent generated by the photosensors. The light can be generated inside the droplet due to both chemiluminescent reactions and excitation of labeled or naturally fluorescent molecules. Moreover, the light variation can be due to the optical absorption from the liquid droplet of an external radiation in label-free detection systems.

Furthermore, the photosensors aligned with the micro-channel can monitor the chemiluminescent reactions [25] as well as bioluminescent reactions. Using an external radiation source and eventually an optical filter that can be integrated with the thin film photodiodes, both fluorescence and absorption measurements can be carried out.

The system comprises also a compact and modular electronic system composed of three electronic boards connected together to control and to interface the electrowetting device with a computer.

3. Design of the microfluidic system and of the a-Si:H photosensors

This design sets the geometrical sizes of the microfluidic system and the active area and pitch of the photosensor array.

3.1. Design of the EWOD electrodes and capillary-driven channel

The area and pitch of the electrodes have been designed taking into account the size of the liquid droplet to move and the minimum distance between them to achieve a successful movement induced by the EWOD technique. In our case the droplet to move is a 2 µl solution. From the experiments we found that this liquid quantity, poured on our hydrophobic layer, covers a circular area with a diameter of 1.7 mm. On the other hand, from literature results it is well known that the distance between the EWOD electrodes has to be less than 70 µm. Therefore we designed our EWOD electrodes as squares with $1.5 \times 1.5\ mm^2$ area and a pitch of 1.56 mm. In this way a droplet can cover two adjacent electrodes, making successful the operation of the EWOD technique.

In order to achieve an efficient coupling of the continuous microfluidics with the EWOD system, we set width, height and length of the microchannel equal to 2 mm, 0.150 mm and 30 mm, respectively,

3.2. Design of the photosensor array

The structure of a single photosensor is a stack of ITO/a-SiC:H *p*-type/a-Si:H intrinsic/a-Si:H *n*-type/metal layers, whose thicknesses and optical properties have been optimized to achieve a low dark current and high responsivity in the visible range [29]. Area and pitch of the linear photosensor array pitch have been designed to maximize the detection of the radiation coming from the drop aligned with the sensor and to minimize the inter-site crosstalk. These two parameters have been investigated applying, to the

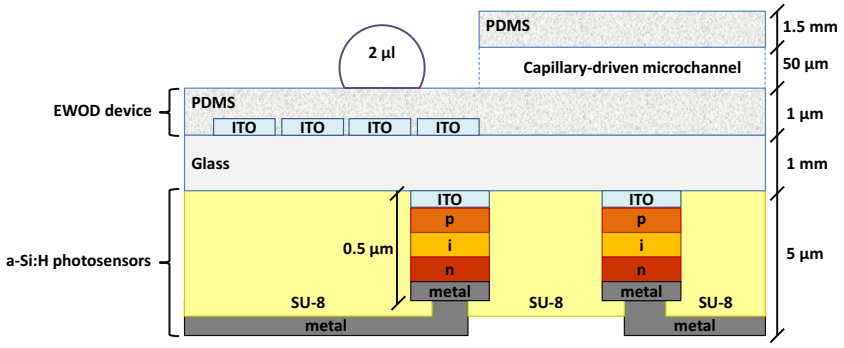

Fig. 1. Cross section of the presented LoC.

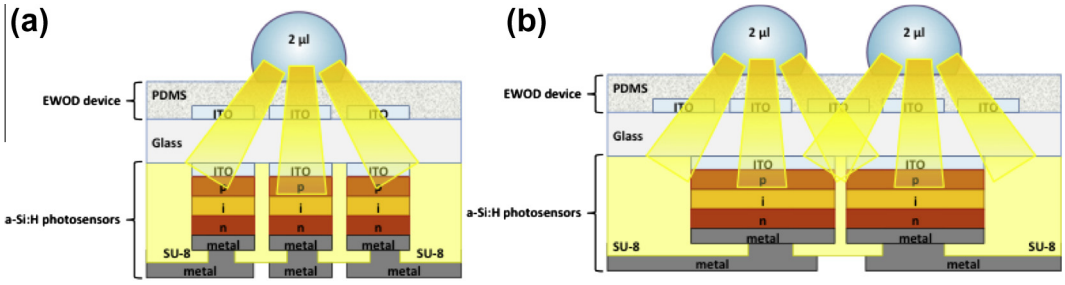

Fig. 2. (a) Structure utilized for maximizing the power impinging on the photosensors. (b) Picture of the optimized structure: the EWOD electrodes have area and distance equal to 1.5 × 1.5 mm^2 and 60 µm, respectively; the photosensors have area and distance equal 2.5 × 2.5 mm^2 and 200 µm, respectively.

structure depicted in Fig. 2a, the model we have developed in [8], where the fraction of the emitted radiation impinging on the photodiode is related to the viewing angle of the sensor with respect to the droplet. The photosensor aligned with the EWOD electrode covered by the droplet receives the useful power, while the other two photosensors located at its sides receive the inter-site power.

We considered a 2-dimensional structure, where the droplet is divided into small regions acting as independent light sources. The light impinging on the three photosensors, calculated as the linear superimposition of the light due to each of the not interacting sources, takes into account:

a) The view angles of the photosensors.
b) The reflections at the interfaces water/hydrophobic layer, hydrophobic layer/ITO, ITO/glass and glass/ITO.
c) The contribution to the light coming from the reflection at the ITO/glass interface due to the first reflection at the glass/ITO interface.

The model assumes a monochromatic light at 550 nm. The refractive indices of the ITO, the hydrophobic layer and the glass at this wavelength have been measured with a Lambda 950 Perkin Elmer Spectrophotometer, while the refractive index of the water has been assumed equal to 1.33.

In the simulation reported below, the droplet has a rectangular shape with base equal to 1.5 mm and height equal to 0.89 mm. In this way, considering squared electrodes, the volume of the droplet is equal to 2 µl. In Fig. 3, the ratio between the power impinging on the central electrode and the total power emitted by the independent light sources as a function of the sensor size is reported as solid circles (left graph side).

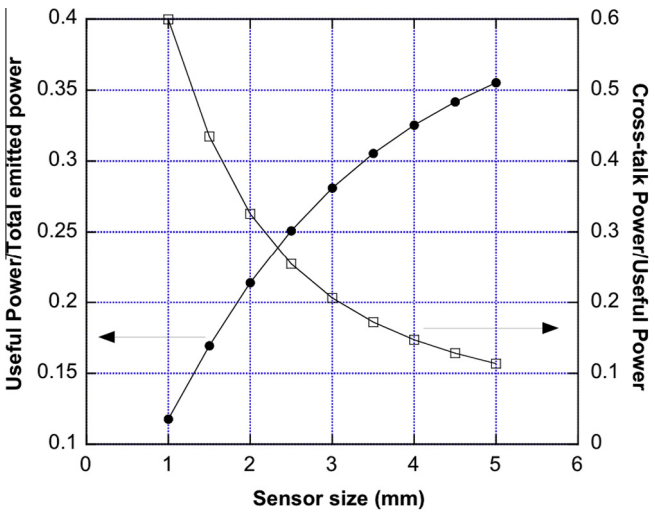

Fig. 3. Fraction of the power impinging on the photosensor (left side, closed symbols) and crosstalk signal (right side, open symbols).

From the figure we see that if the sensor size is equal to the drop size (1.5 mm) the light impinging on the detector is quite low (17% of the total emitted light). Therefore, even though this approach could be interesting, because allows to monitor all the electrodes, it does not give an optimization of the light received by the photosensors.

Increasing the sensor size the useful power increases, but on the other hand the number of sensors that can be placed in correspondence to the EWOD electrodes decreases. From geometrical considerations, we set the sensor size to 2.5 mm with a pitch of 2.7 mm. This configuration (reported in Fig. 2b) enables us to monitor one EWOD electrode every two and to achieve a useful power equal to 25% of the total emitted power.

The effect of this choice on the crosstalk is shown in the right side of Fig. 3. The open symbols represent indeed the ratio between the inter-site power and the useful power as a function of the sensor size with distance between two photosensors set to 200 µm. We observe that the selected geometry (sensor size equal to 2.5 mm) guarantees a inter-site signal four times lower than the useful one and, at the same time, we see that the one photosensor-one EWOD electrode geometry shows an unacceptable crosstalk. Sensor sizes larger than 2.5 mm improve both the useful signal and the crosstalk, but decrease in a significant way the number of monitored electrodes.

4. Structure and operation of the electronics

The electronic board controls and interfaces the LoC system with a computer in order to achieve the droplet movement in the EWOD system. It is composed by two main parts connected in a compact and modular system:

1. A switching board, hosting a microcontroller, that distributes, in the required time sequence, the voltage to the electrodes.
2. A low-power high-voltage generator that, starting from the 5 Volts of a computer USB connection, generates the voltage (ranging from 10 Volts up to 250 Volts) to be supplied to the electrodes.

A graphical unit interface (GUI) developed in C++ controls all the parameters to be sent to the microcontroller through a USB connection.

4.1. Switching board

The switching board is connected to the EWOD system by means of an edge card connector, which guarantees both electrical continuity between board and glass and the electrical insulation between adjacent contacts when the high voltage, supplied by the variable voltage generator, is applied to the electrodes. The

electronic circuit of the main board includes an array of switches (photoMOS relays) and a microcontroller which rules the switch activation timing, controls the functionalities of the variable voltage generator and handles the data communication with the computer via USB interface. Each electrode of the EWOD device is connected to a couple of switches whose status can be set in order to connect the electrode to high voltage, ground potential or floating potential. Detailed description and electrical characterization of this board can be found in [8].

4.2. Low-power high voltage generator board

This board generates a voltage from 10 V up to 250 V starting from the standard 5 V USB power supply without exceeding the maximum current consumption of 500 mA allowed by the USB standard.

The first part of the circuit is a fly-back converter that raises the 5 V input voltage from a computer USB port up to 300 V. The operating principle of the fly-back converter is schematically reported in Fig. 4. When the switch is closed, the transform stores the magnetic energy in its primary coil that is instantly transferred to the secondary coil of the transformer when the switch is opened. This effect produces a current pulse that through a rectifier charges the capacitor "C" generating a high voltage drop across the capacitor.

The standard fly-back circuit [30] has been modified in order to limit the current, provided by the USB port, to 40 mA. However, this restriction increases the charging time of the capacitor. In order to overcome this problem, a rechargeable battery has been connected in parallel to the flyback converter to supply the initial extra-current. In this way, the charging time to the maximum voltage 300 V is lower than 60 s. When the capacitor is charged, since the current needed to actuate the electrowetting electrodes is less than 100 μA, the flyback converter is disconnected from the battery and connected to the USB power supply. During this operating time the battery is recharged from the USB connection.

The output voltage of the flyback converter is the power supply (Vcc) of the voltage regulator circuit (see Fig. 5). This circuit provides an output voltage whose value depends on the output voltage of the Digital to Analog Converter (DAC).

The DAC output voltage ranges from 0 to 4.096 V and its value is controlled by the microprocessor included in the switching board through a feedback loop. The actual output voltage value is acquired by the Analog to Digital Converter (ADC) embedded in the microprocessor. The microprocessor actuates an iterative successive approximation procedure, which changes the value of the DAC voltage until the difference between the required and the actual output voltage is below 1 V. The required output voltage is set through the GUI graphical interface.

The operating principle of the voltage regulator circuit is the following. The DAC voltage is buffered to avoid coupling effect with the transistor Q3 and it is reported to the voltage divider made of resistors R0, R4 and R2//R3. The current flowing through the resistors R0 and R4, up to a negligible current driven by the Darlington couple of transistors Q3 and Q4, flows in the resistor R2// R3 and generates the output voltage. The switch "SW1" (see Fig. 5) allows to change the gain (V_{OUT}/V_{DAC}) of the circuit by connecting the resistor R5 in parallel with the resistors R2 and R3 and thus changing the value of the voltage divider. Taking into account

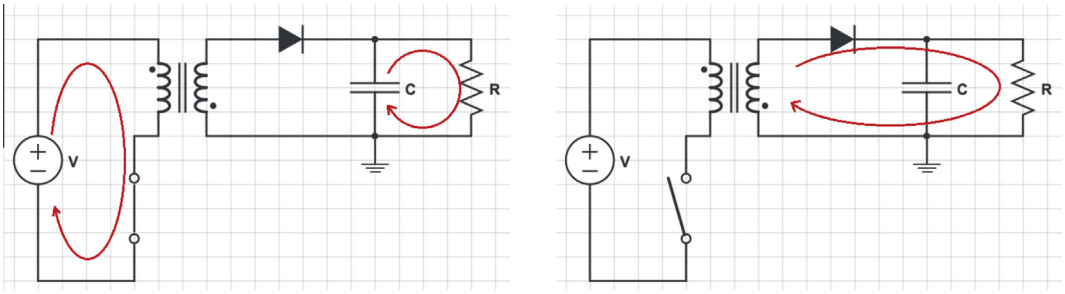

Fig. 4. Schematic representation of the fly-back circuit operation. The voltage generator V is provided by the USB port, while the voltage across the capacitor C drives the EWOD electrodes.

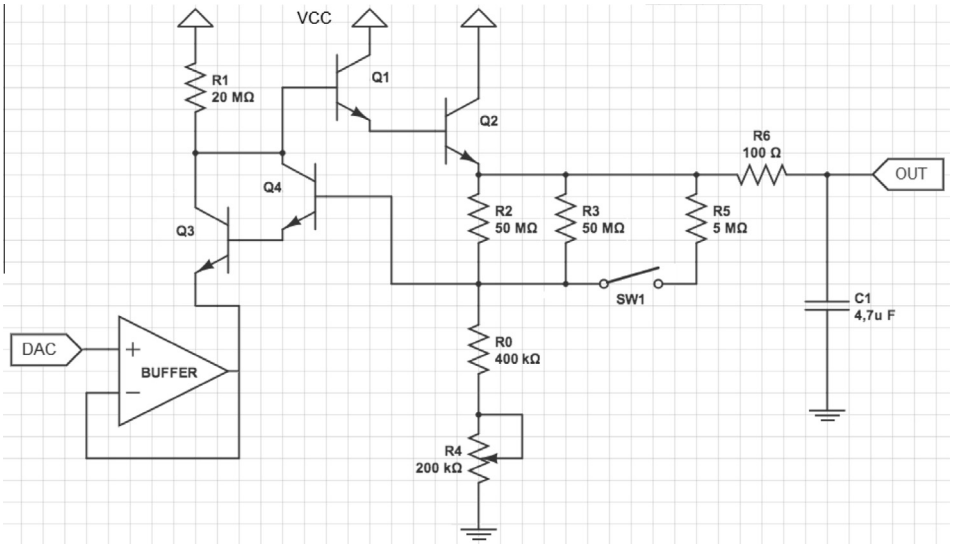

Fig. 5. Voltage regulator circuit Vcc is provided by the flyback circuit, while the output voltage (OUT) depends on the DAC output voltage.

the value of the resistors reported in the circuit of Fig. 5, when the switch is opened the gain V_{OUT}/V_{DAC} is 42.66 and the output voltage range is 45–250 V. When the switch is closed, the gain decreases down to 9.5 and the range is 9–49 V.

We found that the output voltage range is 10–250 V with step of 1 V and ripple less than 40 mV in the entire range of variation.

5. Lab-on-Chip fabrication

The LoC system is fabricated on a glass substrate by using thin film processes. The process sequence takes into account the compatibility of all the technological steps used to fabricate the EWOD electrodes, the a:Si:H photosensors and the capillary-driven microchannels.

5.1. EWOD system

The electrodes of the EWOD structure have been fabricated depositing by magnetron sputtering a 180 nm thick Indium Tin Oxide (ITO) layer. Taking into account the area occupied by a 2 μl droplet, as discussed in Section 3.1, the ITO film has been patterned with a dry etching as a linear array of 7 electrodes with 1.5×1.5 mm^2 distance between them of 60 μm. As reported in [3], a PDMS layer (Rhodorsil RTV 90700 from Siliconi, Padova, Italy) deposited by spin-coating acts as both hydrophobic and insulating layer of our EWOD system. The resulting thickness is 1.3 μm and the contact angle measured at 0 V is 104°.

The droplet used in the experiment reported below is constituted by mineral water. This droplet is enough conductive to enable the fluid movement and at the same time has a low surfactant concentration to avoid the hampering of the movement due to the decrease of the contact angle variation.

5.2. a-Si:H photosensor array

The fabrication process of the photosensors has been performed after the definition of the EWOD electrodes. It requires four lithographic steps, four wet etchings and two dry etchings. To avoid damaging of the EWOD electrodes, they have been protected with a 1.5 μm thick AZ1518 photoresist cured at 115 °C for 3 min.

The a-Si:H photosensors are ITO/a-SiC:H *p*-type/a-Si:H intrinsic/a-Si:H *n*-type/metal stacked structures. A 180 nm-thick ITO layer, which acts as transparent bottom contact of the diodes, has been deposited by magnetron sputtering and patterned by dry etching process (mask 1). Then, the a-Si:H stacked structure *p*-type/intrinsic/*n*-type has been deposited by Plasma Enhanced Chemical Vapor Deposition (PECVD). The deposition parameters of the a-Si:H layers are reported in [29].

A three-metal Cr/Al/Cr stack, which acts as top contact of the sensors, has been deposited by vacuum evaporation. Then, the photosensors area have been defined by wet etching (mask 2) of the Cr/Al/Cr stack and subsequently by the mesa patterning by dry etching of the a-Si:H layers (mask 2). As suggested by the simulations, the area of the photosensors has been set to 2.5×2.5 mm^2. In order to insulate the top and the bottom layers of the photosensors, a 5 μm-thick SU8 (from Micro-Chem, MA, U.S.A.) passivation layer has been deposited by spin coating and via the holes over the diodes patterned by wet etching (mask 3). Finally, a 150 nm-thick titanium/tungsten alloy layer has been deposited by sputtering and subsequently patterned (mask 4) for the definition of the top grid electrodes and of the connection to the pad.

5.3. Capillary-driven microfluidic channel

The capillary-driven microchannel fabrication is the last technological step. Its dimensions are $3\text{ cm} \times 2\text{ mm} \times 150\ \mu\text{m}$ ($L \times W \times H$). The PDMS used to fabricate the microchannel was the Sylgard184 from Dow Chemicals with a 1:10 ratio between the curing agent and the base elastomer. The technological procedure for the fabrication is described below. The mold for the PDMS channel has been fabricated overlapping on a glass holder two sheets of 75 μm thick Kapton tape and shaping them with the channel dimensions. The two components of PDMS have been mixed and the bubbles removed by gentle vacuum. Then, the mixed PDMS has been poured into the holder obtaining a PDMS structure 1.5 mm thick. Finally, the PDMS has been cured at 80 °C for 90 min. The described steps produce a PDMS channel with hydrophobic surfaces, which are not suitable for a capillary-driven microfluidic device as the one to be coupled with the electrowetting device. The hydrophilic characteristic of the channel, indeed, is a strict requirement to generate the capillary pressure, which drives the liquid movement inside the channel. Therefore, we have treated the internal surfaces of the microchannel with Poly Ethylene Glycol (PEG), which turns the walls of the channel from hydrophobic into hydrophilic type changing the PDMS wetting characteristics. In order to achieve hydrophilic surfaces we exposed the internal walls of the PDMS to oxygen plasma for 30 s. Then, we diluted 0.2 g of PEG in 0.2 ml of deionized water and we poured the solution over the treated walls of the channel. Finally, the PDMS structure was thermal cured at 150 °C for 90 min and rinsed in deionized water to remove the excess of PEG.

6. Results and discussion

The functionality and successful integration of the different fabrication processes have been verified with three different tests:

a. Detection through the array of the amorphous silicon photosensors of a droplet over an EWOD electrode;
b. Integration of the capillary-driven microfluidics with the EWOD system.

The operation of the device has been evaluated moving a water droplet forward and backward over an EWOD electrode and monitoring the current of the corresponding photosensor when a radiation is impinging over the LoC system from the EWOD glass side. A 2 μl water droplet has been spotted on the PDMS and moved by the EWOD system by applying 200 V between two adjacent electrodes. Thanks to the transparent electrodes, the light reaches the photodiodes and generates a photocurrent signal, which is modulated by the presence of the droplet. Photosensor currents have been measured in three different droplet positions: far (a), close (b) and over (c) the electrode as reported in the upper part of Fig. 6. Data of the figure report the histograms of the current values corresponding the three droplet positions in multiple experiments performed at different times. We see that these positions can be easily distinguished confirming that the a-Si:H photosensors are effective in detecting the presence of a droplet over the electrode.

The presented experiment is a proof of principle of the effectiveness of a-Si:H photosensors to monitor a variation of light over the electrodes. However, the PDMS over the EWOD electrodes could be functionalized [31] in order to immobilize bioreceptors and recognize different analytes contained in drops transported over the electrodes. The subsequent transport of other solutions can give rise to luminescent phenomena detected by the photosensors.

With this integration a drop of solution transported by the EWOD system to the inlet of the microfluidic channel flows inside the microchannel. Depending on its composition and residence time, the injected solution can functionalize the glass [32] inside the microchannel, immobilize bioreceptors and recognize different

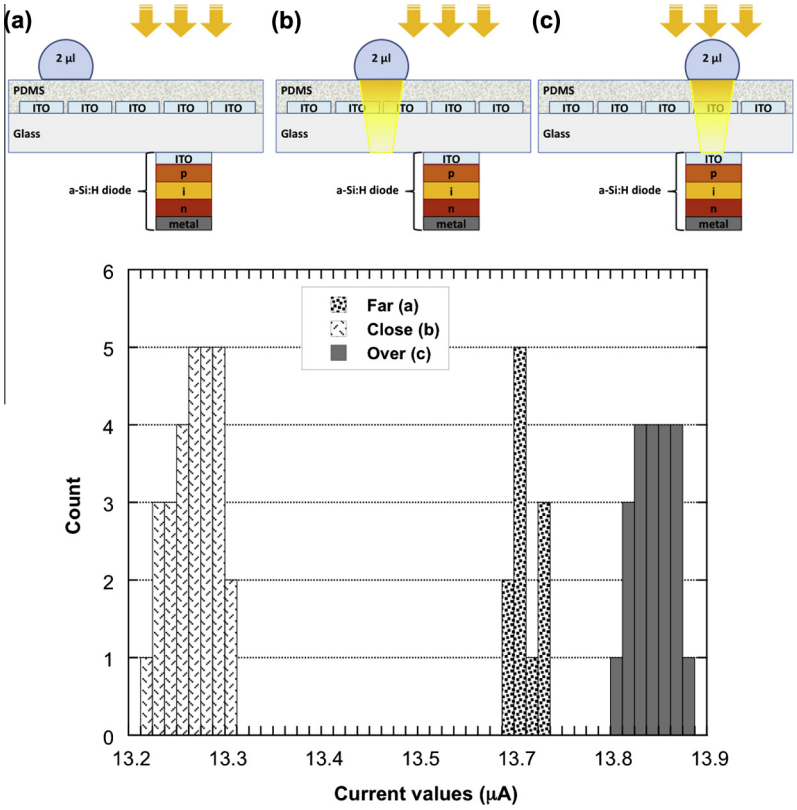

Fig. 6. Histogram of the current values flowing in a a-Si:H photosensor, when the droplets is in three different positions over the EWOD system: (a) 6 mm from the monitored electrode (far), (b) 1 mm from the monitored electrode (close), (c) over the monitored electrode.

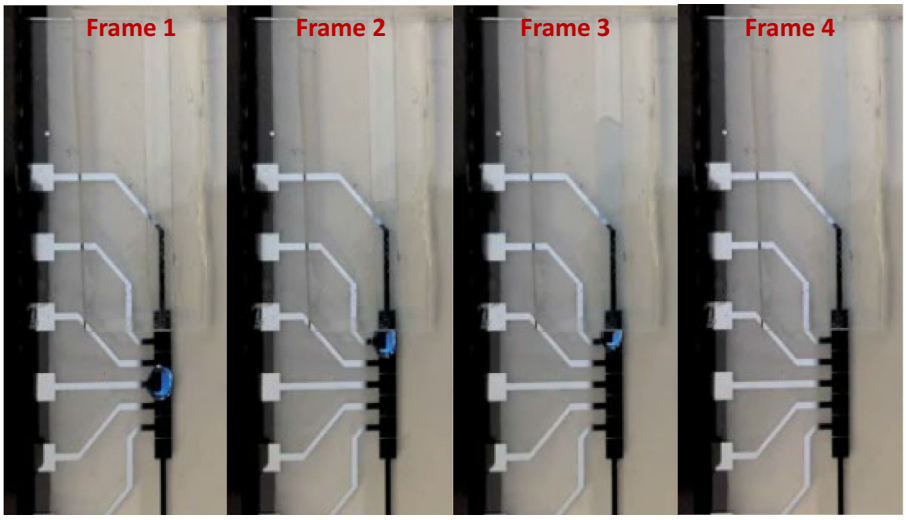

Fig. 7. Frames of a movie demonstrating the drop movement and the microchannel filling.

biomolecules on the functionalized surface. The geometry and fabrication of the EWOD system are the ones described in Section 5.1, except for the material of the EWOD electrodes, that is a 30 nm/200 nm/30 nm Cr/Al/Cr metal layer stack deposited by magnetron sputtering and patterned by wet etching. The reason for this change is to demonstrate the possibility to achieve a correct operation of the EWOD system with different thin film technologies.

The capillary-driven microchannel has been fabricated in PDMS as described in Section 5.3 and then placed on the EWOD device aligned with the last electrode of the array. A 2 µl water droplet has been spotted on the PDMS of the EWOD structure and moved actuating the electrodes towards the inlet of the microchannel. When the droplet reached the inlet of the channel, the hydrophilic characteristic of the inner walls drives the liquid to the outlet of the channel. Fig. 7 reports four frames captured during the experiment. Frames 1 and 2 demonstrate the movement toward the microchannel inlet, while frames 3 and 4 the filling of the capillary-driven microchannel.

7. Conclusions

A LoC system which combines, on the same glass substrate, on-chip fluidic handling and on-chip detection has been designed, fabricated and tested. The on-chip fluidic handling comprises both digital microfluidic based on the EWOD technique and continuous flow microfluidic based on capillary-driven microfluidic channels. The on-chip detection is performed by an array of a-Si:H photosensors, whose low deposition temperature (around 250 °C) enables the use of standard glass substrate.

The optimization of the useful light impinging on the photosensors and the minimization of the crosstalk have ruled the design of the geometrical sizes of both the EWOD electrodes and of the photosensor array. The compatibility of the technological steps has ruled instead the sequence of the microelectronic thin film processes for the fabrication of the whole Loc system.

The correct functionality of the integrated technological parts has been successful verified showing that the proposed LoC presents the features of a "true" Lab-on-Chip system, avoiding off-chip detection units as well as microfluidic interconnections toward pumps or syringes.

Conflict of interest

The authors declare that they have no conflict of interest.

Acknowledgements

Authors would like to thank the financial support of the European Community's Seventh Framework Programme FP7-SME-2013 "DEMOTOX" – Proposal no 604752, the Center for Life Nano Science@Sapienza, Istituto Italiano di Tecnologia (Rome, Italy) and the Italian Ministry of Education, University and Research (MIUR) through PRIN2010-2011 project "ARTEMIDE" and the University Project Research 2013 – prot. C26A13HKFB "Lab-on-Chip system for mycotoxin detection in food commodities".

Appendix A. Supplementary data

Supplementary data associated with this article can be found, in the online version, at http://dx.doi.org/10.1016/j.sbsr.2014.10.010.

References

[1] A.G. Crevillen, M. Hervas, M.A. Lopez, M.C. Gonzalez, A. Escarpa, Real sample analysis on microfluidic devices, Talanta 74 (3) (2007) 342–357.
[2] T.M.H. Lee, M.C. Carles, I.M. Hsing, Microfabricated pcr-electrochemical device for simultaneous dna amplification and detection, Lab Chip 3 (2) (2003) 100–105.
[3] D. Caputo, M. Ceccarelli, G. de Cesare, A. Nascetti, R. Scipinotti, Lab-on-glass system for dna analysis using thin and thick microtechnologies, MRS Proceedings, 1191, Cambridge Univ Press, 2009. 1.
[4] S. Haeberle, R. Zengerle, Microfluidic platforms for lab-on-a-chip applications, Lab Chip 7 (2007) 1094–1110.
[5] D. Mark, S. Haeberle, G. Roth, F. von Stetten, R. Zengerle, Microfluidic lab-on-a-chip platforms: requirements, characteristics and applications, Chem. Soc. Rev. 39 (2010) 1153–1182.
[6] F. Costantini, A. Nascetti, R. Scipinotti, F. Domenici, S. Sennato, L. Gazza, F. Bordi, N. Pogna, C. Manetti, D. Caputo, G. de Cesare, On-chip detection of multiple serum antibodies against epitopes of celiac disease by an array of amorphous silicon sensors, RSC Adv. 4 (4) (2014) 2073–2080.
[7] M. Washizu, Electrostatic actuation of liquid droplets for micro-reactor applications, IEEE Trans. Ind. Appl. 34 (4) (1998) 732–737.
[8] D. Caputo, G. de Cesare, N. Lovecchio, A. Nascetti, R. Scipinotti, Electrowetting-on-dielectric system based on polydimethylsiloxane, Proceedings of the 5th IEEE IWASI, 99–103, POD Publ: Curran Associate, Inc., 2013.
[9] B. Shapiro, H. Moon, R.L. Garrell, C.J. Kim, Equilibrium behavior of sessile drops under surface tension, applied external fields, and material variations, J. Appl. Phys. 93 (9) (2003) 5794–5811.
[10] A.T. Pereira, A.C. Pimentel, V. Chu, D.M.F. Prazares, J.C. Conde, Chemiluminescence detection of horseradish peroxidase using an integrated amorphous silicon thin film photosensor, IEEE Sens. J. 9 (2009) 1282–1290.
[11] C.H. Liu, Y.C. Chang, T.B. Norris, Z. Zhong, Graphene photodetectors with ultra broadband and high responsivity at room temperature, Nature Technol. 9 (2014) 273–278.
[12] X. Wang, M. Amatatonchai, D. Nacapricha, O. Homann, J.C. de Mello, D.D.C. Bradley, A.J. de Mello, Thin film organic photodiodes for integrated on-chip chemiluminescent detection – application to antioxidant capacity screening, Sens. Actuators B Chem. 140 (2009) 643–648.
[13] N.M. Matos Pires, T. Dong, U. Hanke, L. Holvik, Integrated optical microfluidic biosensor using a polycarbozole photodetector for point-of-care detection of hormonal compounds, J. Biomed. Opt. 18 (2013) 097001.
[14] G. de Cesare, M. Gavesi, F. Palma, B. Riccò, A novel a-Si:H mechanical stress sensor, Thin Solid Films 427 (1) (2003) 191–195.
[15] D. Caputo, G. de Cesare, New a-Si:H two terminal switching device for active display, J. Non-Cryst. Solids 198–200 (1996) 1134–1137.
[16] D. Caputo, G. de Cesare, A. Nascetti, M. Tucci, Detailed study of amorphous silicon ultraviolet sensor with chromium silicide window layer, IEEE Trans. Electr. Dev. 55 (1) (2008) 452–456.
[17] R. Martins, P. Baptista, L. Raniero, G. Doria, L. Silva, R. Franco, E. Fortunato, Amorphous/nanocrystalline silicon biosensor for the specific identification of unamplified nucleic acid sequences using gold nanoparticle probes, Appl. Phys. Lett. 90 (2007) 023903. 1/023903-3.
[18] D. Caputo, G. de Cesare, A. Nascetti, R. Negri, R. Scipinotti, Amorphous silicon sensors for single and multicolor detection of biomolecules, IEEE Sens. J. 7 (2007) 1274–1280.
[19] D. Caputo, G. de Cesare, C. Manetti, A. Nascetti, R. Scipinotti, Smart thin layer chromatography plate, Lab Chip 7 (2007) 978–980.
[20] F. Fixe, V. Chu, D.M.F. Prazeres, J.P. Conde, An on-chip thin film photodetector for the quantification of DNA probes and targets in microarrays, Nucleic Acids Res. 32 (2004) e70–e75.
[21] G. de Cesare, D. Caputo, A. Nascetti, C. Guiducci, B. Riccò, Hydrogenated amorphous silicon ultraviolet sensor for deoxyribonucleic acid analysis, Appl. Phys. Lett. 88 (2006) 083904. 1/083904-3.
[22] D. Caputo, G. de Cesare, A. Nascetti, R. Negri, Spectral tuned amorphous silicon p-i-n for DNA detection, J. Non-Cryst. Solids 352 (2006) 2004–2007.
[23] D. Caputo, G. de Cesare, C. Fanelli, A. Nascetti, A. Ricelli, R. Scipinotti, Amorphous silicon photosensors for detection of Ochratoxin A in wine, IEEE Sens. J. 12 (8) (2012) 2674–2679.
[24] A. Joskowiak, V. Chu, D.M.F. Prazeres, J.P. Conde, Amorphous silicon photosensors for detection of intrinsic cell fluorophores, MRS Proceedings, 1321, Cambridge University Press, 2011, pp. 435–439. 1.
[25] D. Caputo, G. de Cesare, L.S. Dolci, M. Mirasoli, A. Nascetti, A. Roda, R. Scipinotti, Microfluidic chip with integrated a-Si:H photodiodes for chemiluminescence-based bioassays", IEEE Sens. J. 13 (2013) 2595–2602.
[26] A.C. Pimentel, A.T. Pereira, V. Chu, D.M.F. Prazeres, J.P. Conde, Detection of chemiluminescence using an amorphous silicon photodiode, IEEE Sens. J. 7 (2007) 415–416.
[27] D. Caputo, G. de Cesare, R. Scipinotti, N. Stasio, F. Costantini, C. Manetti, A. Nascetti, On chip diagnosis of celiac disease by an amorphous silicon chemiluminescence detector, Lect. Notes Electr. Eng. 268 (2014) 183–187.
[28] R.B. Fair, Digital microfluidics: is a true lab-on-a-chip possible?, Microfluid Nanofluid. 3 (2007) 245–281.
[29] D. Caputo, G. de Cesare, A. Nascetti, R. Scipinotti, Amorphous silicon photosensors for on-chip detection in digital microfluidic system, Sens. Actuators A Phys. 216 (2014) 1–6.
[30] Billings, Keith, Switchmode Power Supply Handbook, second ed., McGraw-Hill, 1999. ISBN 0-07-006719-8.
[31] J. Zhou, A.V. Ellis, N.H. Volcker, Recent developments in PDMS surface modification for microfluidic devices, Electrophoresis 31 (2010) 2–16.
[32] F. Costantini, R. Tiggelaar, S. Sennato, F. Mura, S. Schlautmann, F. Bordi, H. Gardeniers, C. Manetti, Glucose level determination with a multi-enzymatic cascade reaction in a functionalized glass chip, Analyst 138 (17) (2013) 5019–5024.